CHAPTER IV

POWER SPECTRA ANALYSIS OF BUBBLE FREQUENCY

4.1 Introduction

The porosity or concentration fluctuation and bubble frequency measurements are important from the point of view of erosion of fluidized bed combustor heat transfer tubes. Baumgarten and Pigford (1960) used the radiation densitometer for porosity fluctuation measurements. Recently, Gidaspow (1986) used the γ-ray densitometer to measure porosity fluctuations in gas-solid fluidized beds. Gidaspow et al. (1988) used a spectral analysis program in conjunction with an IBM compatible personal computer to analyze the porosity fluctuation data. Figure 4.1 (Gamwo, 1992) illustrates the setup developed for the porosity measurements for gas-solid fluidized bed experiments. This unit was used previously by other researchers (Gidaspow et al, 1983; Gamwo and Gidaspow, 1992) for experiments conducted at the Illinois Institute of Technology, Chicago.

In this chapter, the concentration fluctuations measurements in two-phase and three-phase fluidized beds are described and analyzed. The concentration fluctuation signals were detected by using a γ-ray absorption technique. The frequencies of concentration oscillations at various locations have been analyzed by means of the fast Fourier transform (FFT) power spectrum method.

4.2 Experimental Setup and Procedure

The experimental setup used for porosity acquisition and FFT power spectra

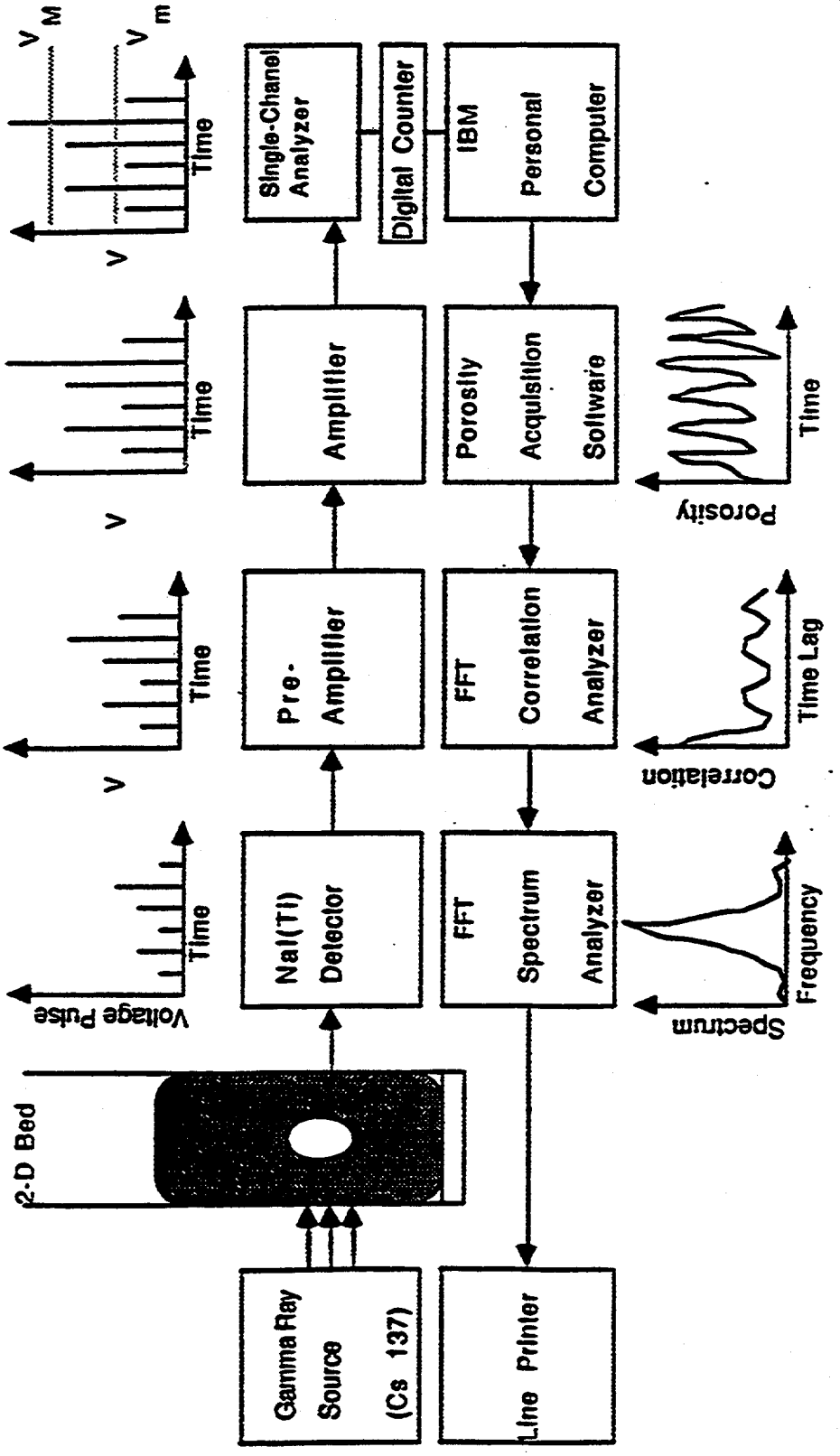

Figure 4.1. Schematic Diagram of Porosity Acquisition System (Gamwo, 1992)

analysis consisted of three major components : the fluidization equipment, a densitometer assembly and an FFT analyzer. The descriptions of the fluidization equipment and the densitometer assembly are given earlier in Chapter 2. A schematic diagram of the experimental setup is shown in Figure 2.1.

4.2.1 Experimental Procedure. The instantaneous porosity fluctuation measurements were made for both the three-phase (gas-liquid-solid) and the two-phase (gas-liquid) fluidized beds. In the experiments, a high speed camera with 60 frames per second was used to record the bubble paths, bubble diameter and bubble velocity. The experimental measurements were taken at many different locations. The dominant frequencies of porosity fluctuations were calculated using the power spectrum analyzer. The experimental procedure used in these measurements is described below.

4.2.1.1 Gas-Liquid-Solid Fluidized Bed. In order to measure concentration fluctuations in the gas, liquid and solid phases, the radiation source and detector were placed at a desired location by moving them horizontally and vertically using built-in tracks. All the measurements were initiated when the air stream was opened while the liquid was continuously flowing into the bed, and the particles were in a fluidized state as a result of liquid flow. The initial bed height was 25.4 cm. Instantaneous readings using an integrator time constant of 0.1 seconds were obtained for a sampling time of 40 seconds and a sampling frequency of 10 Hz.

4.2.2.2 Gas-Liquid Fluidized Bed. The experimental data were recorded at the instant the bed was fluidized by gas while liquid was continuously flowing into the bed. The instantaneous readings using an integrator time constant of 0.01 seconds were

obtained for a sampling time of 40 seconds, and a sampling frequency of 90 Hertz.

4.3 Experimental Concentration Fluctuation and Power Spectra Results

The major results are summarized for experimental measurements at the following three locations :

1. X = 15.24 cm, Y = 3.81 cm,
2. X = 10.16 cm, Y = 12.7 cm,
3. X = 12.7 cm, Y = 12.7 cm.

4.3.1 Gas-Liquid-Solids Fluidized Bed. Figure 4.2 shows the experimental transient concentration fluctuations in a gas-liquid-solids fluidized bed at a location 15.24 cm from the left wall (X) and 3.81 cm from the bottom of solids bed (Y). This location is on the axial centerline of the fluidized bed. Figure 4.3 shows the corresponding power spectra versus frequency diagram. Figure 4.3 shows that there is no dominant frequency indicating an absence of bubble break-up and resulting particles concentration fluctuation. This location is only 3.81 cm (1.5 inches) from the bottom of the bed. The bubbles introduced from the gas-distributor are of only 0.3 cm diameter. These small bubbles are still growing because of coalescence and no bubble break-up is taking place. Figures 4.4 and 4.5 show experimental concentration fluctuation and corresponding power spectra, respectively, at a different location X = 10.16 cm and Y = 12.7 cm. Figure 4.5 shows that there are two dominant frequencies corresponding to 0.56 Hz and 6.2 Hz. The dominant frequencies are related to concentration fluctuations in gas and solids phases, respectively. This location is 12.7 cm (5.0 inches) above the bottom of the bed where

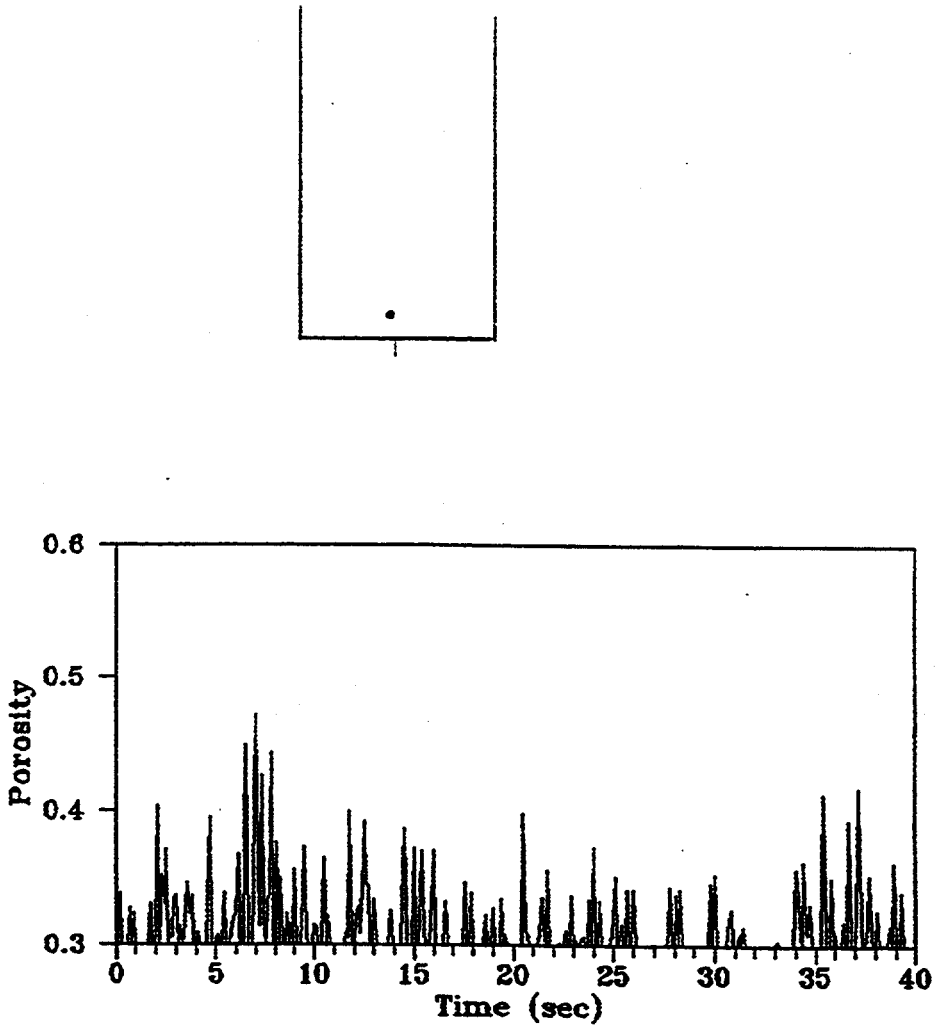

Figure 4.2. Experimental Measurement of Fluctuation of Bubble at X=15.24 cm and Y=3.81 cm for Gas-Liquid-Solid System

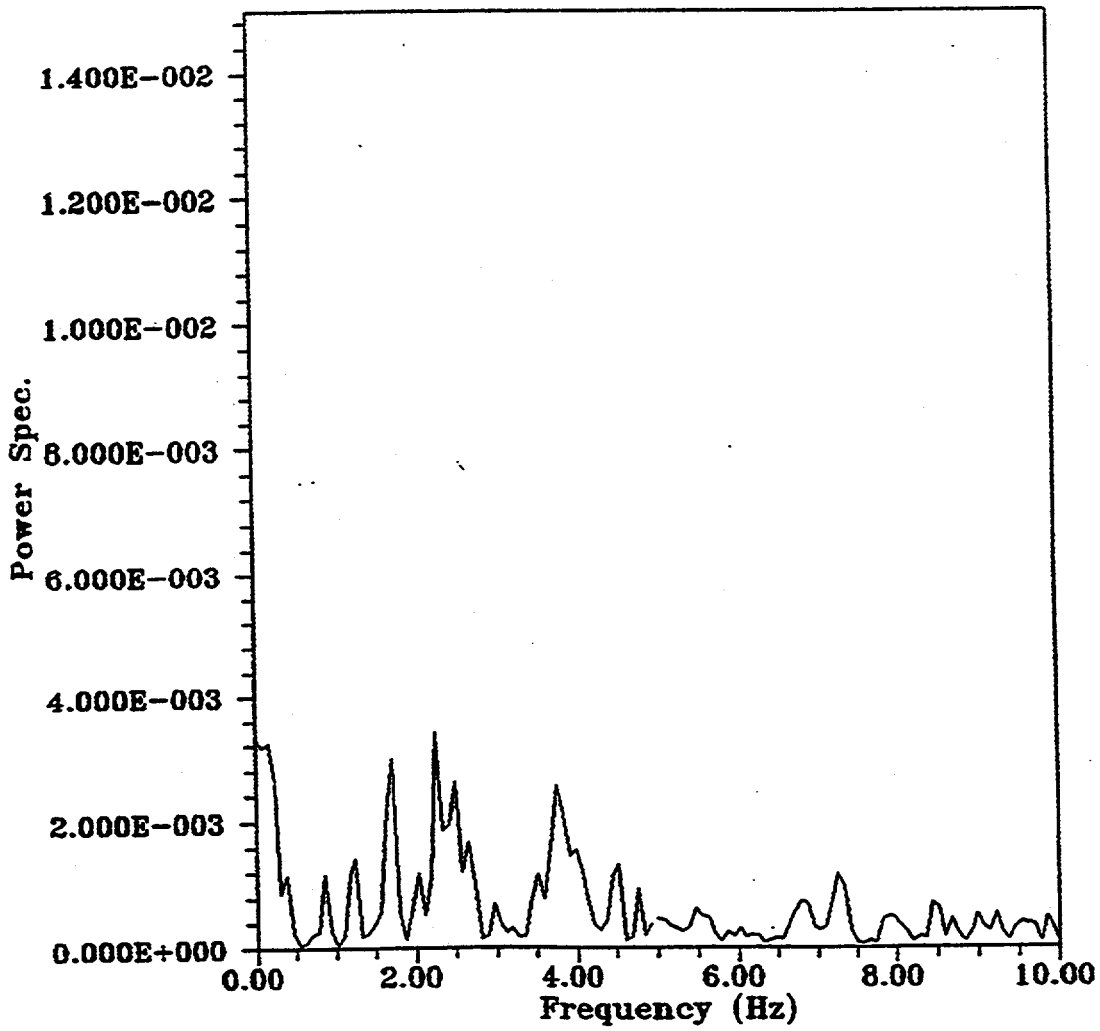

Figure 4.3. Approximated Porosity Power Spectrum at X=15.24 cm and Y=3.81 cm for Gas-Liquid-Solid System

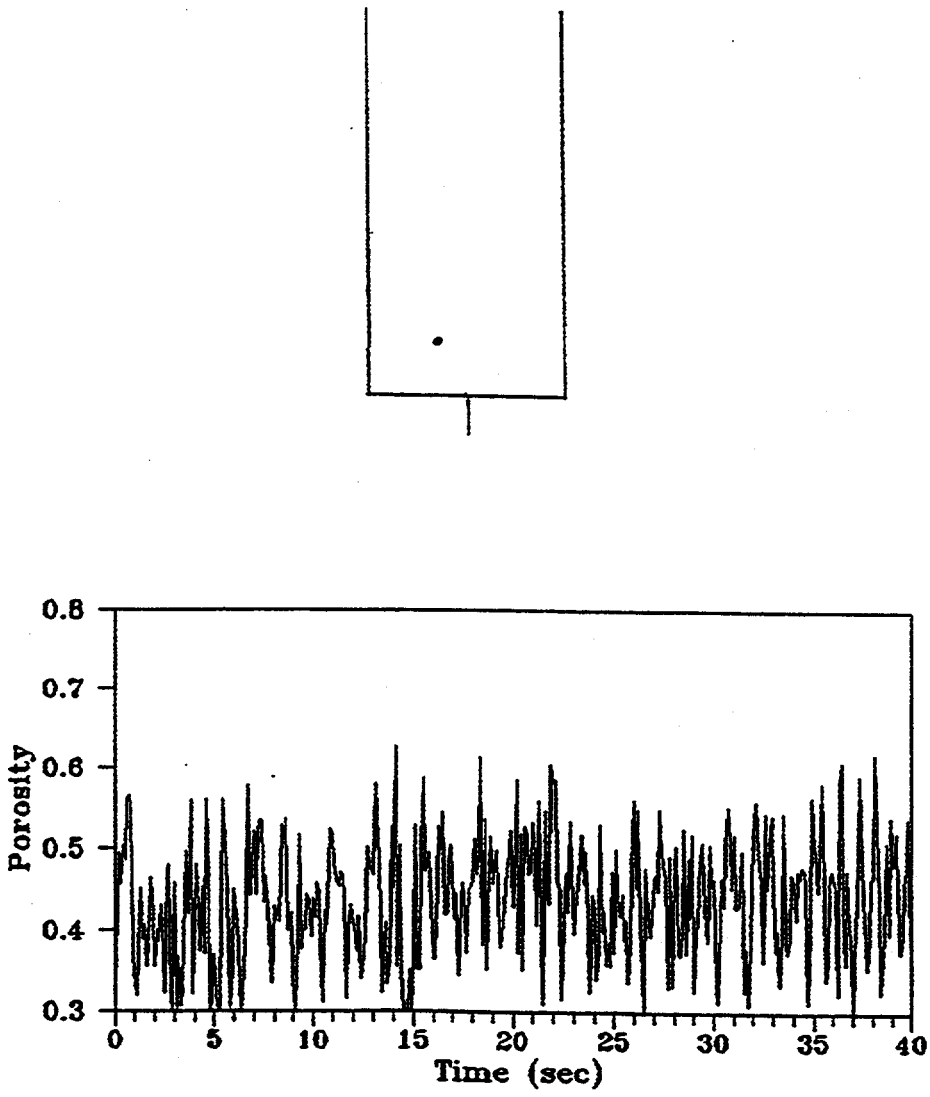

Figure 4.4. Experimental Measurement of Fluctuation of Bubble at X=10.16 cm and Y=12.7 cm for Gas-Liquid-Solid System

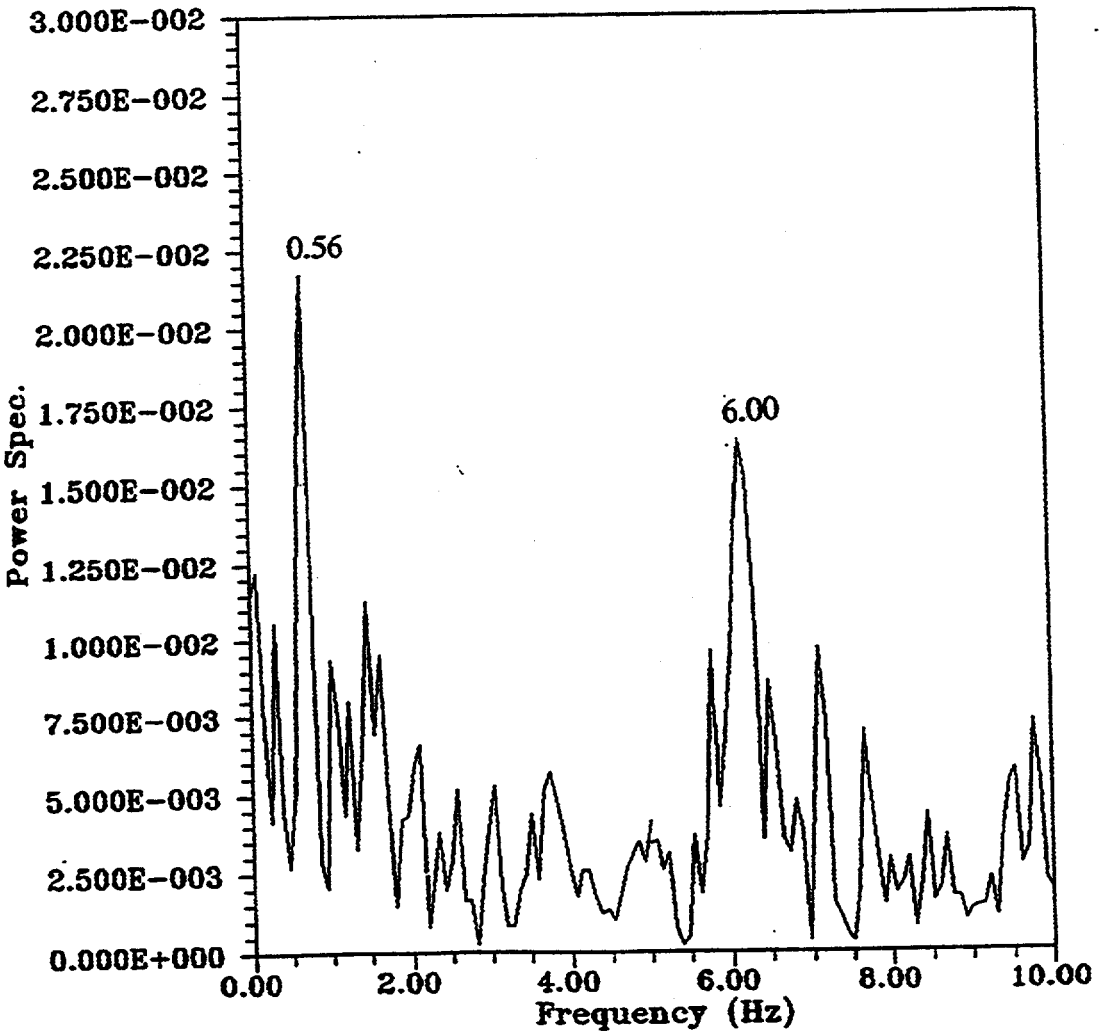

Figure 4.5. Approximated Porosity Power Spectrum at X=10.16 cm and Y=12.7 cm for Gas-Liquid-Solid System

some bubble break-up is already taking place.

Figures 4.6 and 4.7 also show experimental concentration fluctuation and corresponding power spectra, respectively, at a different location X = 12.7 cm and Y = 12.7 cm. This location is at the same height but 2.54 cm (1 inch) left of the previous location. At this location, there seem to be three dominating frequencies at 0.1 Hz, 0.75 Hz and 6.2 Hz. It is plausible that the third frequency at 0.1 Hz is related to the flow behavior and interaction in the center and wall regions of the fluidized bed.

4.3.2 Gas-Liquid Fluidized Bed. The experiments in gas-liquid fluidized bed were conducted to observe the differences in fluidization behavior in the absence of particles. Figures 4.8 to 4.13 show the transient porosity oscillations, and the corresponding power spectra versus frequency plots in a gas-liquid fluidized bed at the same locations where measurements were obtained for the gas-liquid-solids experiments described above.

The power spectra versus frequency at location 1 shown in Figure 4.9 shows no dominant frequency. This situation is similar to that observed in a gas-liquid-solid fluidized bed and confirms the fact that the small bubbles are still growing because of coalescence.

However, Figure 4.11 at location 2 also shows that there is no dominant frequency. In this case, the bubbles are moving up fast in the absence of particles. Thus, a low residence time is available to bubbles, and bubble coalescence is still continuing. Also, there are no particles present to cause bubble break-up. Figure 4.13 at location 3 shows a dominant frequency at 6.0 Hz. In the absence of bubble break-up, the flow interactions

between the center and wall regions of the bed are a likely reason. This interaction is similar to that presented for third dominant frequency in the gas-liquid-solid fluidization experiment. The dominant frequency in a gas-liquid fluidized bed is large signifying a slower rate of interaction.

Overall, the figures show that even though there were interactions between the gas and the liquid phases because of the absence of particles, the disintegration (break-up) of bubbles was occurring at a lower rate in the gas-liquid fluidized bed as compared to those in the three-phase fluidized bed. Also, the bubbles were moving at higher speeds, and larger bubble diameters were developed. Hence, the bubble propagation, collision, and bursting in a fluidized bed generate the void fluctuations.

Although, in a gas-liquid fluidized bed, we visually observed more frequencies of bubbles with larger diameter and faster speed than those in the three-phase fluidized bed, due to the low sensitivity of the detector and the high bubble velocity, Figures 4.8 to 4.13 show that hardly any bubble occurred in those positions.

Figure 4.14 shows the locations where the measurements for porosity oscillations were obtained. The data of major frequencies, seen in Figure 4.14, are also listed in Table 4.1. The dominant frequencies of porosity fluctuations were calculated using the power spectrum analyzer.

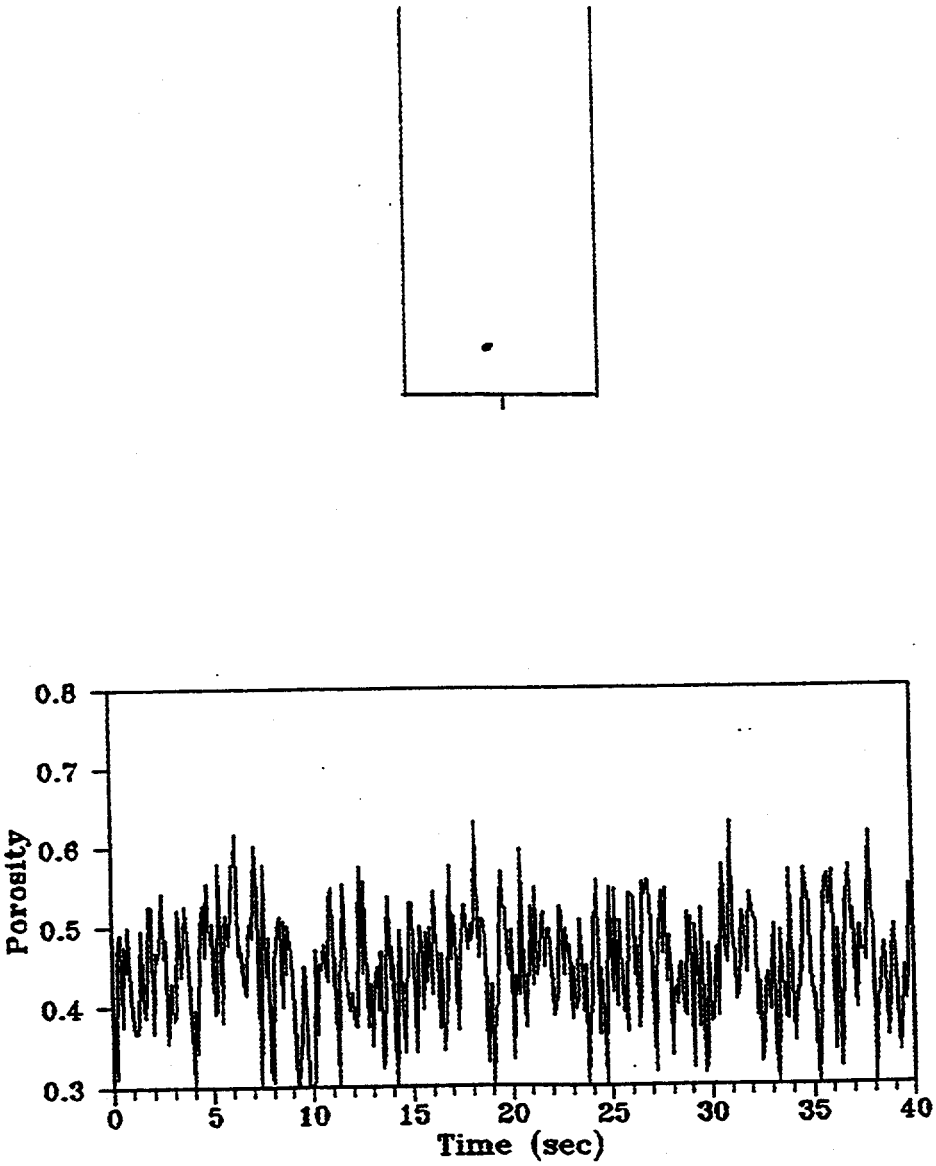

Figure 4.6. Experimental Measurement of Fluctuation of Bubble at X=12.70 cm and Y=12.7 cm for Gas-Liquid-Solid System

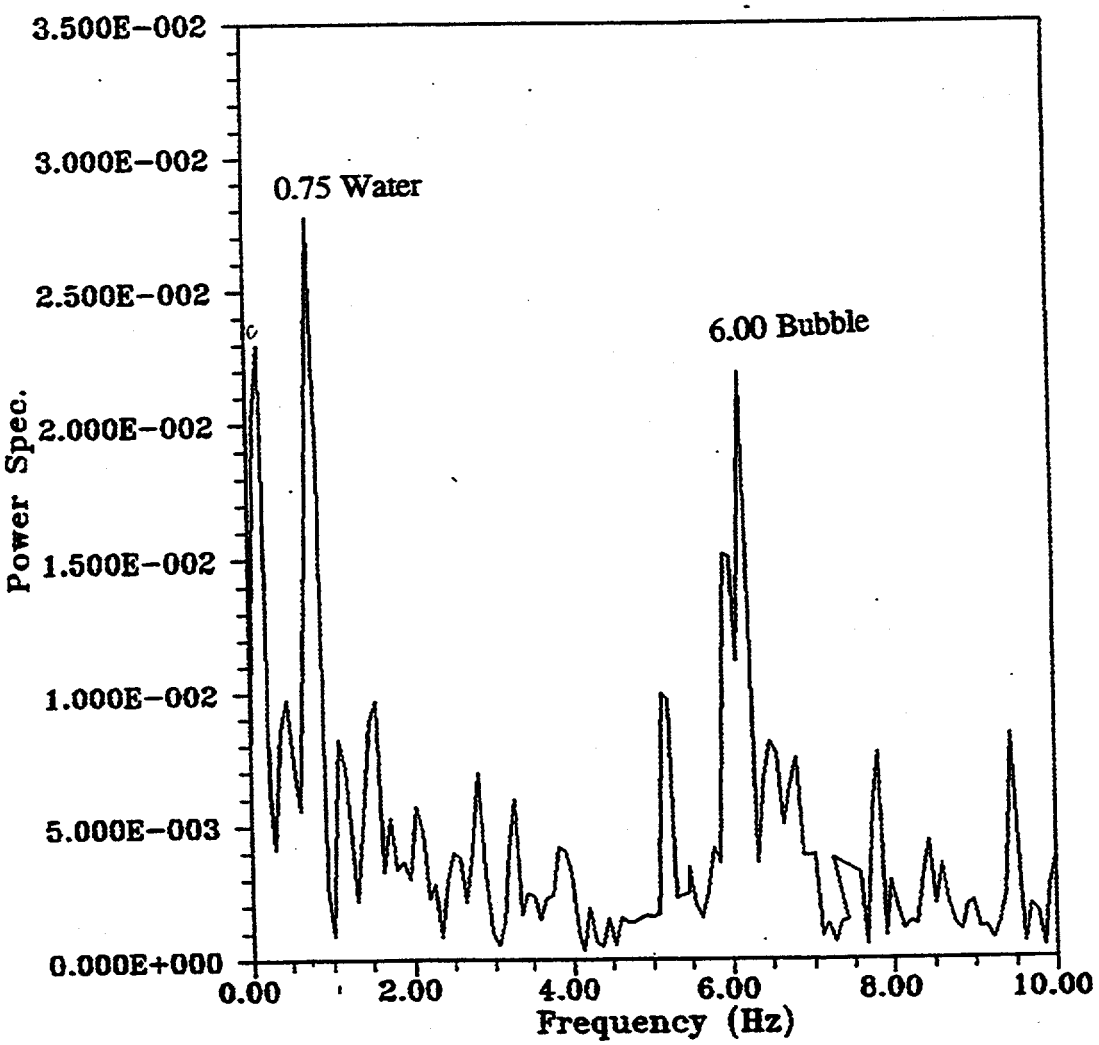

Figure 4.7. Approximated Porosity Power Spectrum at X=12.70 cm and Y=12.7 cm for Gas-Liquid-Solid System

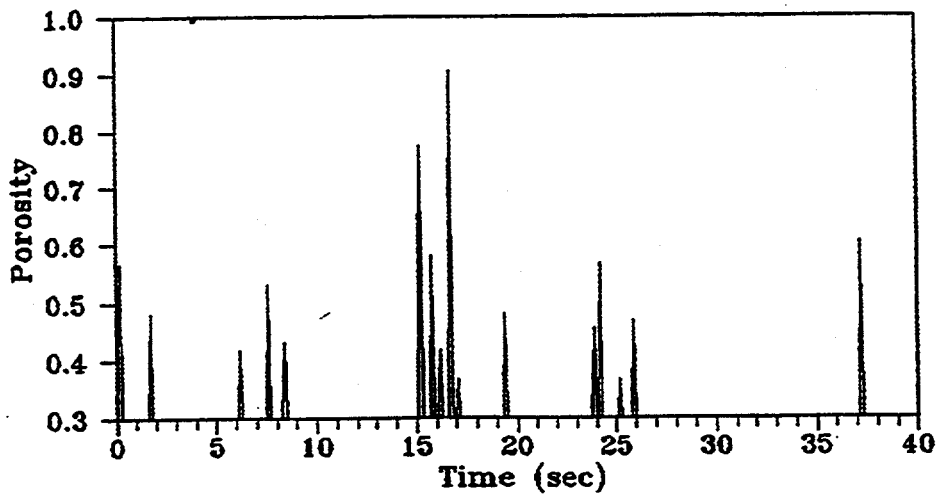

Figure 4.8. Experimental Measurement of Fluctuation of Bubble at X=15.28 cm and Y=3.81 cm for Gas-Liquid System

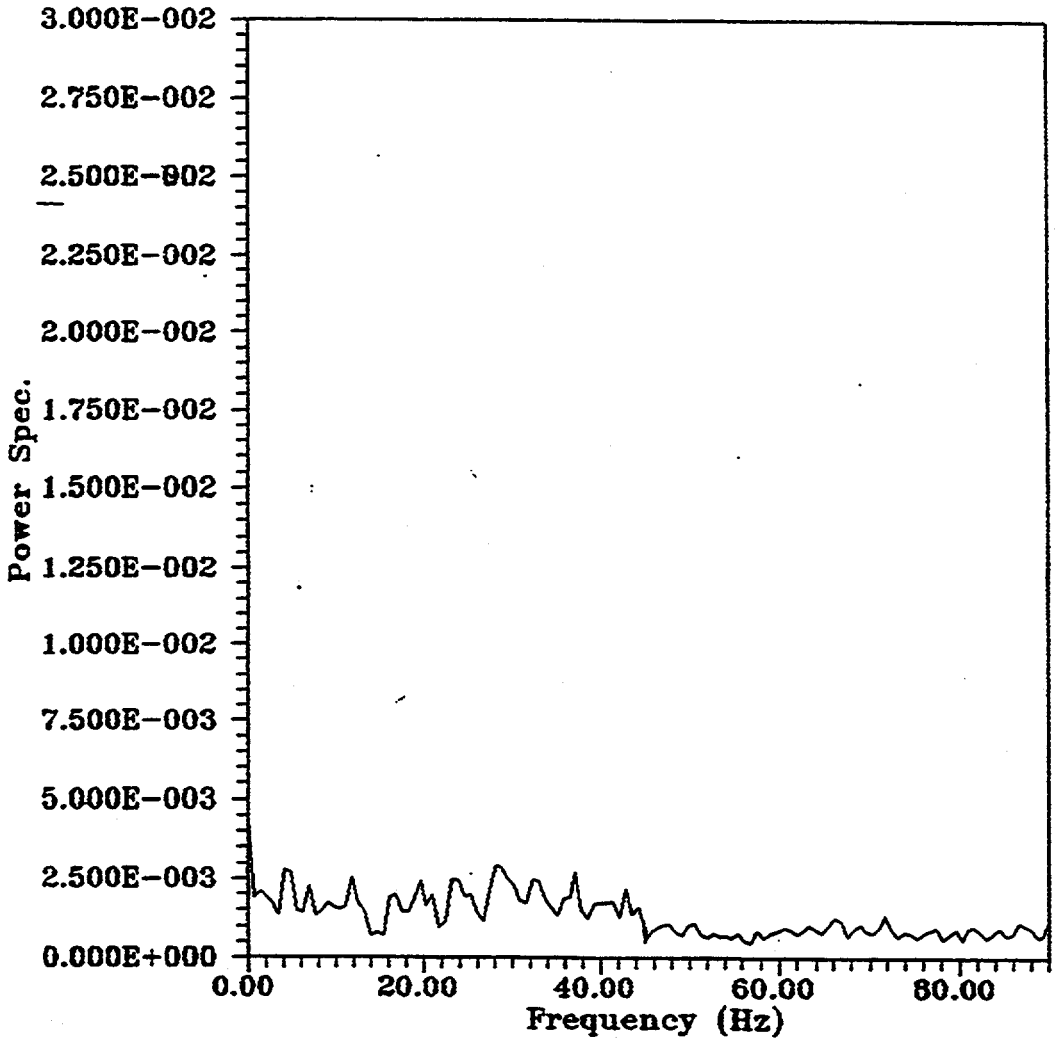

Figure 4.9. Porosity Power Spectrum at X=15.28 cm and Y=3.81 cm for Gas-Liquid System

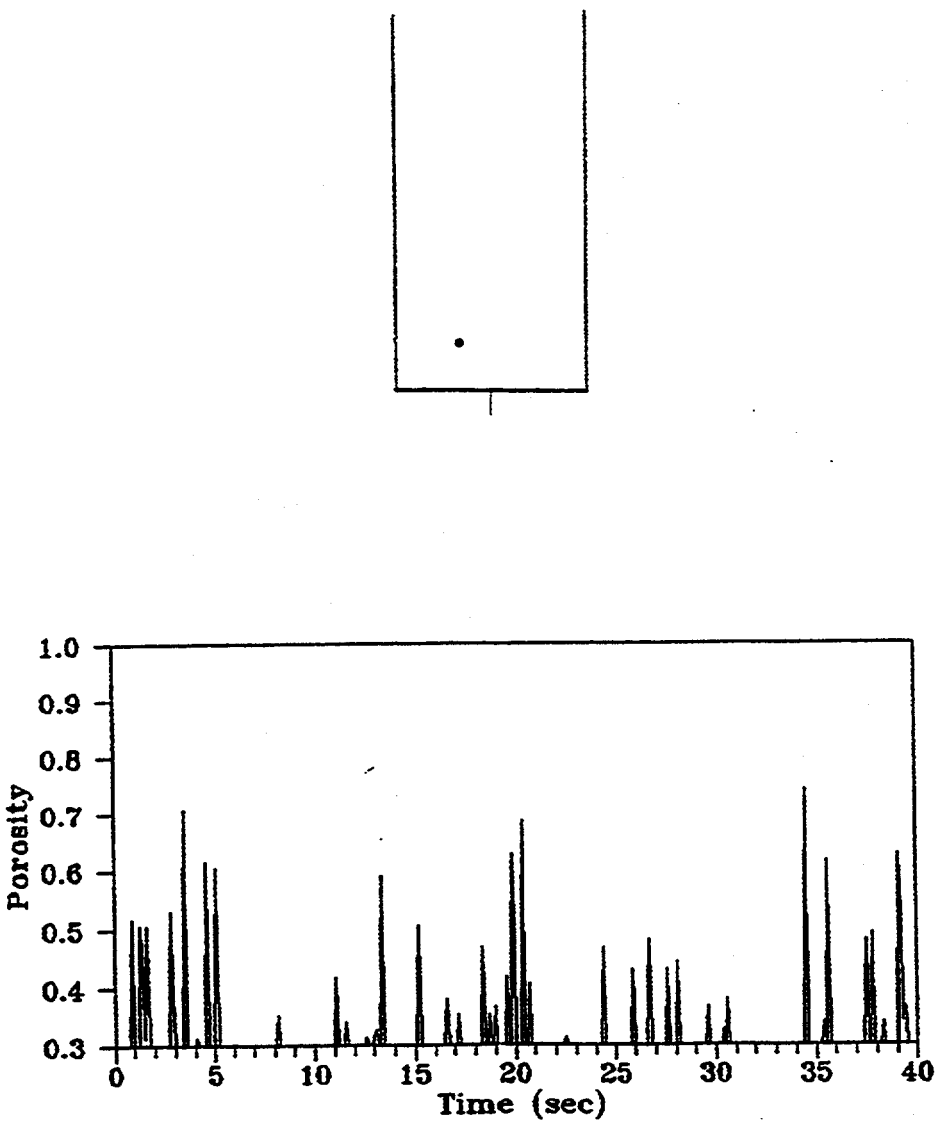

Figure 4.10. Experimental Measurement of Fluctuation of Bubble at X=10.16 cm and Y=12.7 cm for Gas-Liquid System

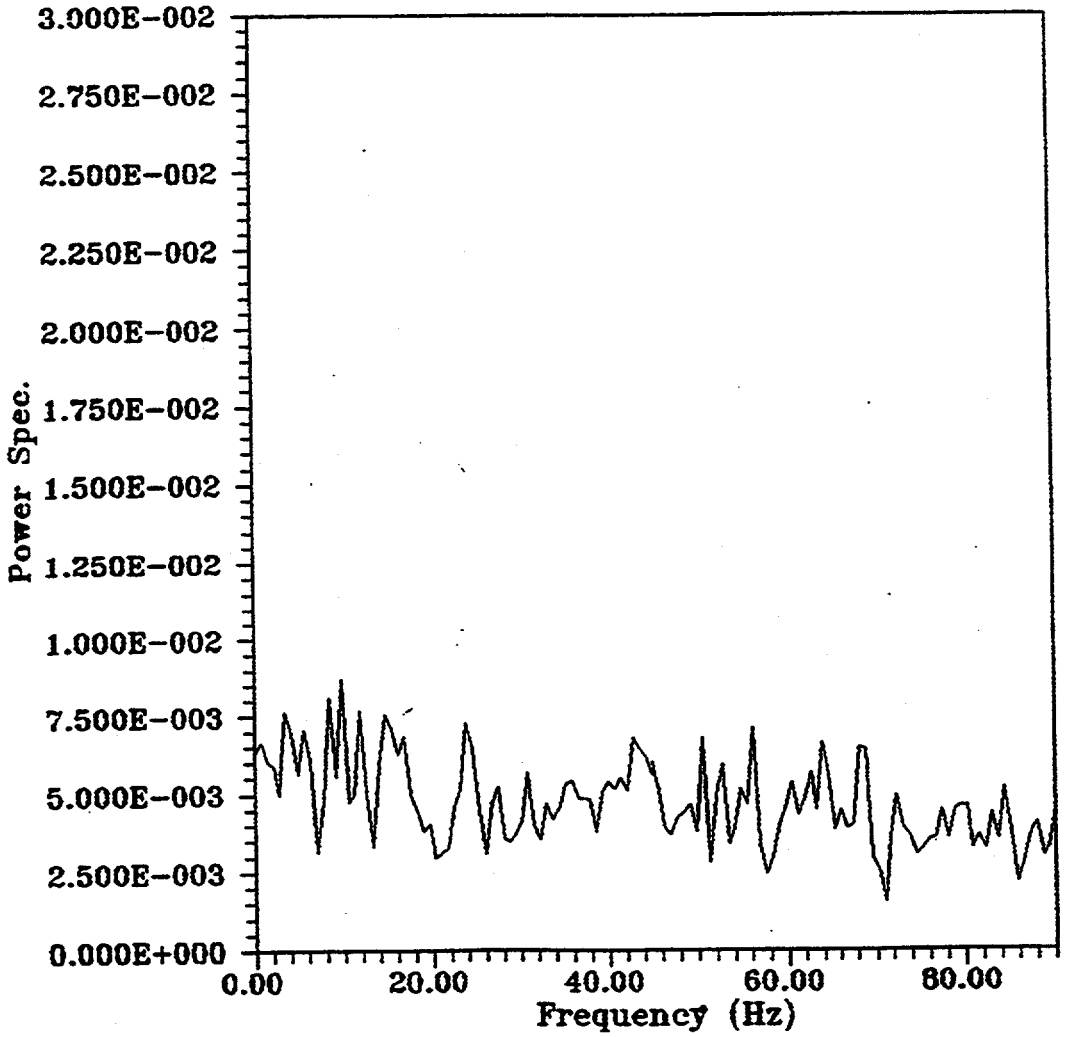

Figure 4.11. Porosity Power Spectrum at X=10.16 cm and Y=12.70 cm for Gas-Liquid System

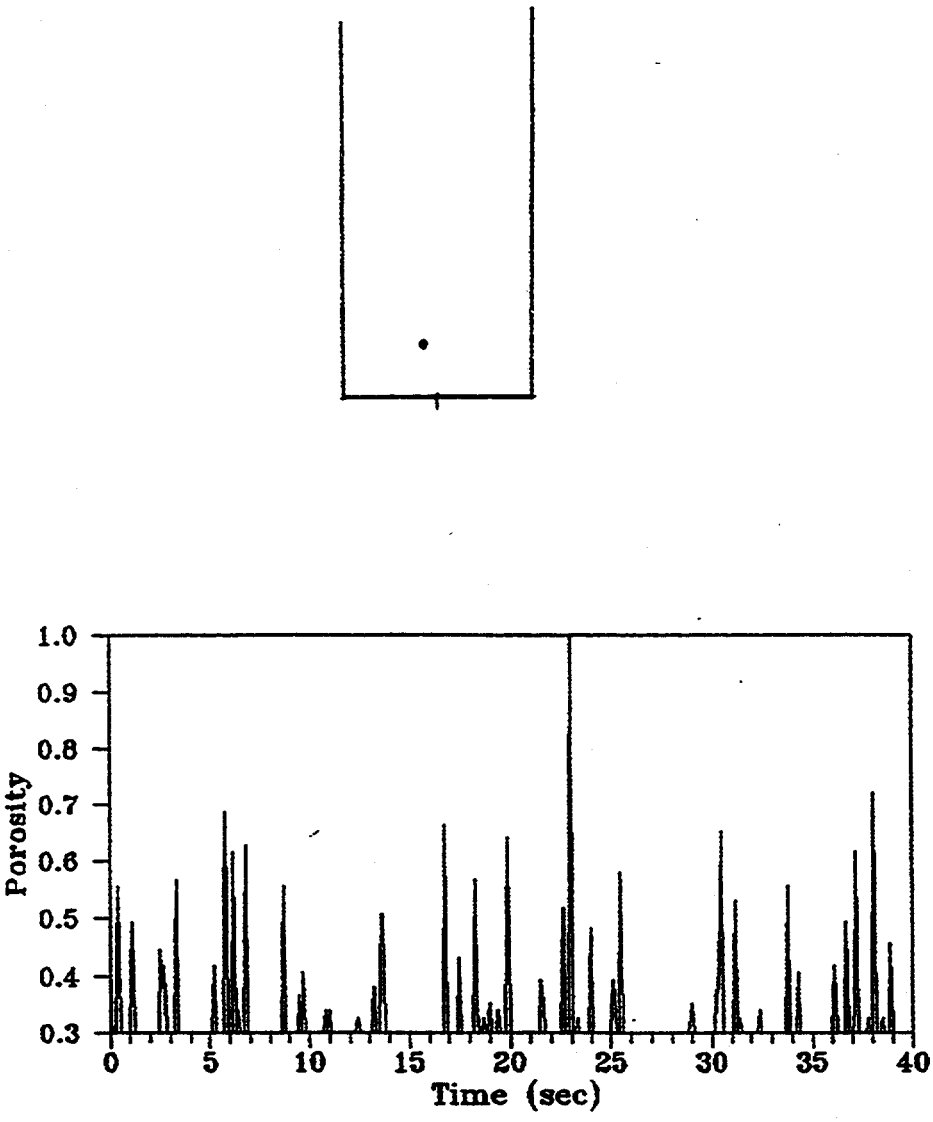

Figure 4.12. Experimental Measurement of Fluctuation of Bubble at X=12.7 cm and Y=12.7 cm for Gas-Liquid System

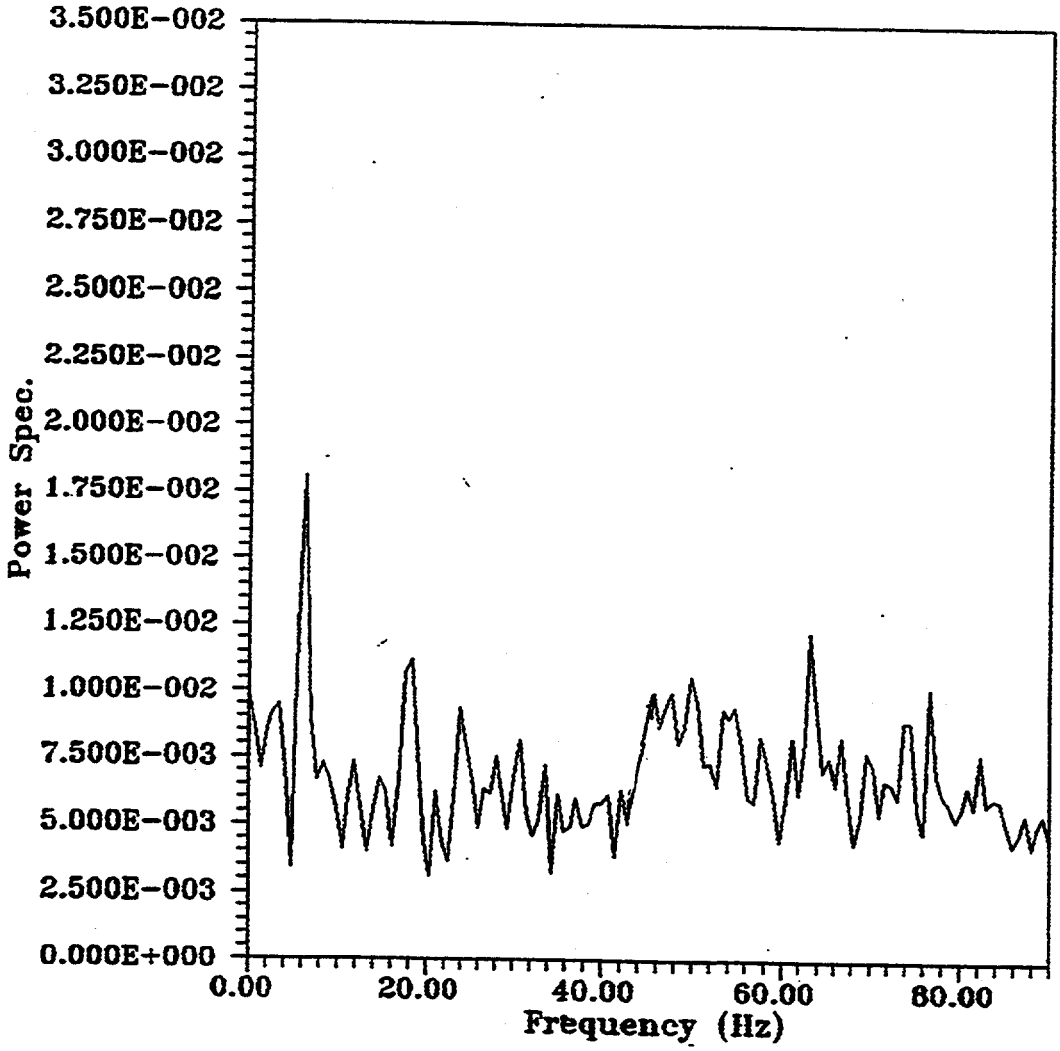

Figure 4.13. Porosity Power Spectrum at X=12.70 cm and Y=12.70 cm for Gas-Liquid System

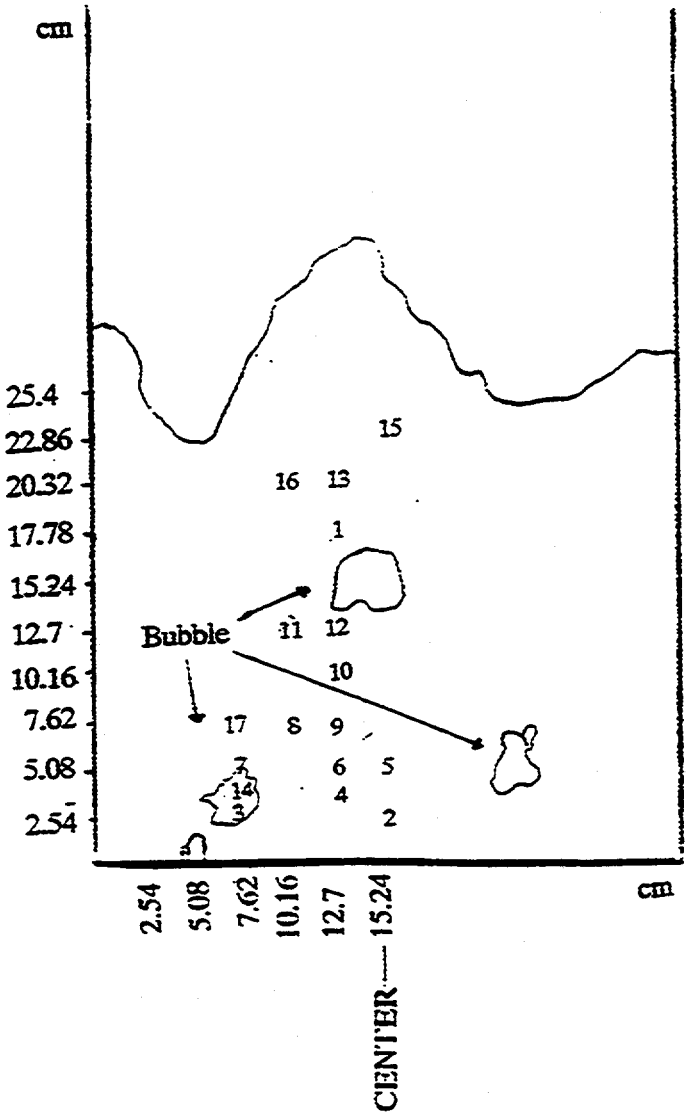

Point	Frequency (Hz)
(1)	—
(2)	—
(3)	0.5,5.4
(4)	—
(5)	0.48,5
(6)	—
(7)	0.75
(8)	—
(9)	—
(10)	8
(11)	0.56,6.2
(12)	0.1,0.75,6.2
(13)	—
(14)	0.3,1.5.6
(15)	—
(16)	—
(17)	—

Figure 4.14. Bubble Frequencies along the Bubble Path

Table 4.1 Bubble Frequencies in Three-Phase Fluidized Bed at Different Locations

Point	Location X (cm)	Location Y (cm)	Frequency (Hz)
1.	12.7	17.78	None
2.	15.24	2.54	None
3.	7.62	2.54	0.5, 5.4
4.	12.7	3.81	None
5.	15.24	5.08	0.48, 5.0
6.	12.7	5.08	None
7.	7.62	5.08	0.75
8.	10.16	7.62	None
9.	12.7	7.62	None
10.	12.7	10.16	8.0
11.	10.16	12.7	0.56, 0.62
12.	12.7	12.7	0.1, 0.75, 6.2
13.	12.7	20.32	None
14.	7.62	3.81	0.3, 1.0, 5.6
15.	15.24	22.86	None
16.	10.16	20.32	None
17.	7.62	7.62	None

4.4 Computed Concentration Fluctuation and Power Spectra Results

The experimental concentration fluctuations were compared with those obtained using hydrodynamic simulations of the fluidized bed. The details of gas-liquid-solids fluidized bed simulations are given in Chapter 7. The computational results shown in this chapter are for the simulations in asymmetric mode.

Figures 4.15 to 4.20 show the computational results of porosity distributions and power spectra diagrams.

In order to evaluate the validity of power spectra analysis, the predicted time-average gas volume fractions shown in the Figure 7.1 were compared with those in the experiment. Figure 7.1(b) shows that the computed time averaged gas volume fraction of gas, at location X = 10.16 cm and Y = 12 cm, is very low, 0.3. As a result, at that location, there is no dominant frequency as seen in Figure 4.18. However, Figures 3.7(b) and 4.5 agreed quite well when the experimental measurements showed that the gas volume fraction at location X = 10.16 cm and Y = 12.7 cm was 0.64. The dominant frequencies of the bubble were 0.58 Hz and 6.2 Hz.

4.5 Conclusion

1. The porosity fluctuations data provided experimentally verifiable results. Such information is useful in designing a fluidized bed with heat transfer tubes.

2. The comparison between experimental and simulation data was fair.

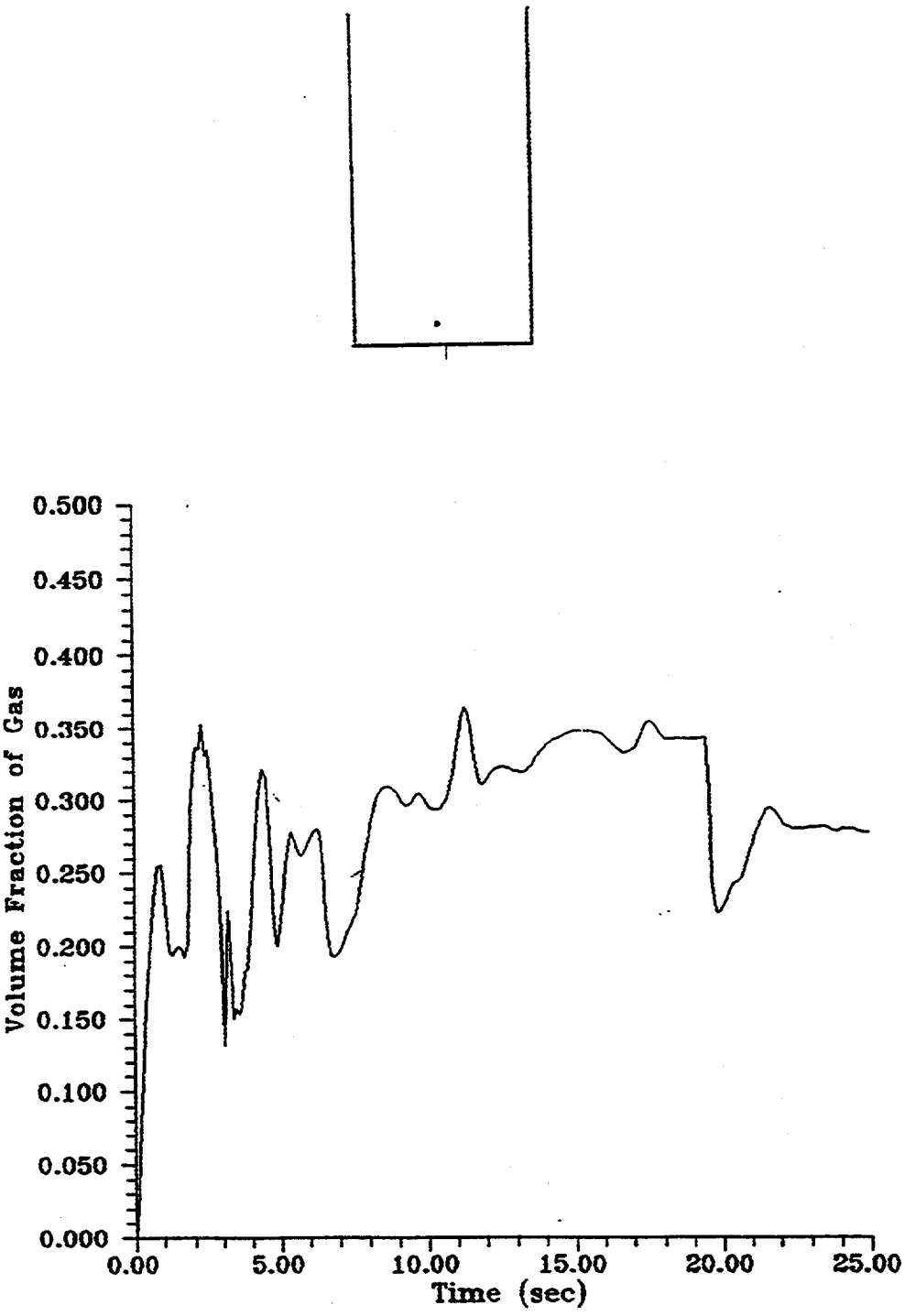

Figure 4.15. Computational data of Fluctuation of Bubble at X=15.28 cm and Y=4 cm for Gas-Liquid-Solid System

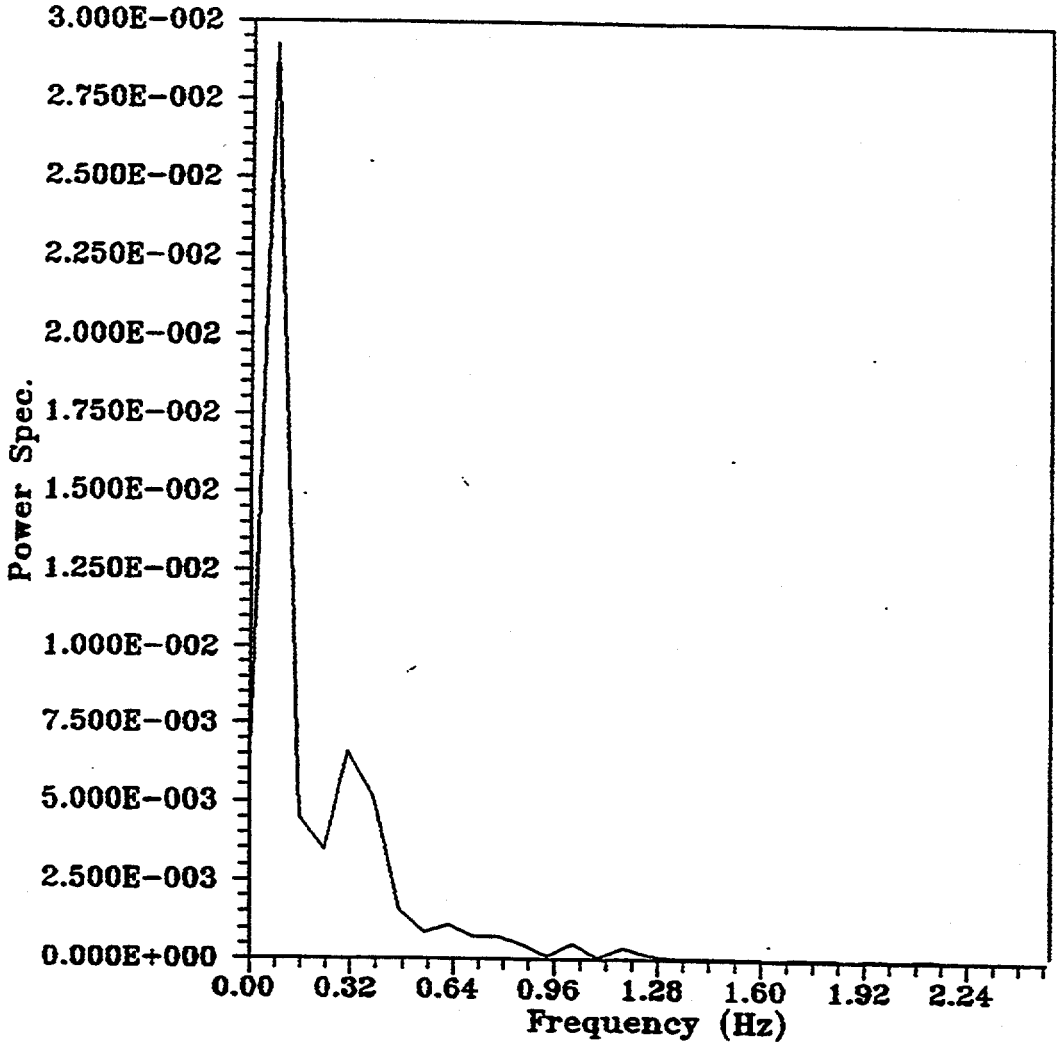

Figure 4.16. Porosity Power Spectrum at X=15.24 cm and Y=4 cm for Gas-Liquid-Solid System

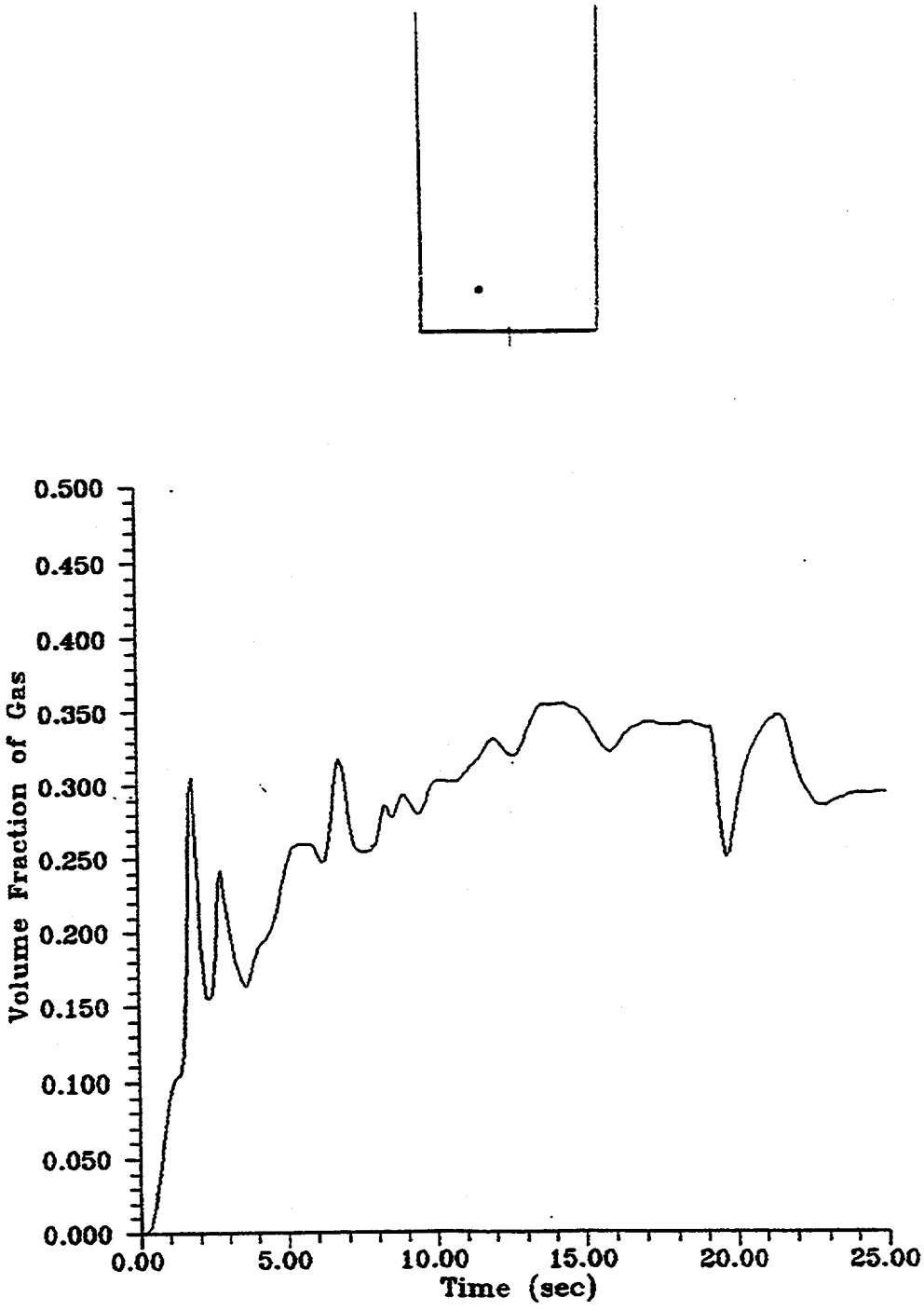

Figure 4.17. Computational data of Fluctuation of Bubble at X=10.16 cm and Y=12 cm for Gas-Liquid-Solid System

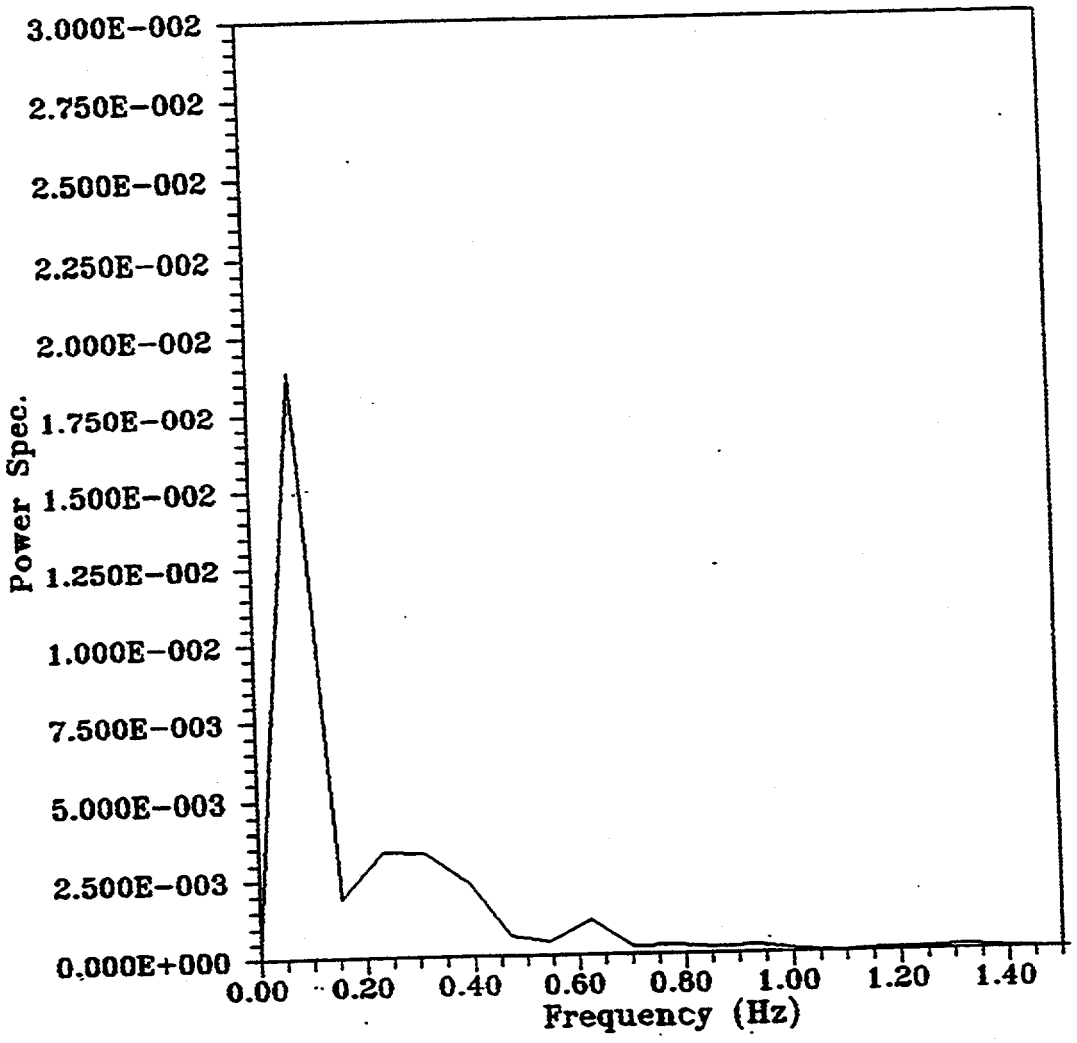

Figure 4.18. Porosity Power Spectrum at X=10.16 cm and Y=12 cm for Gas-Liquid-Solid System

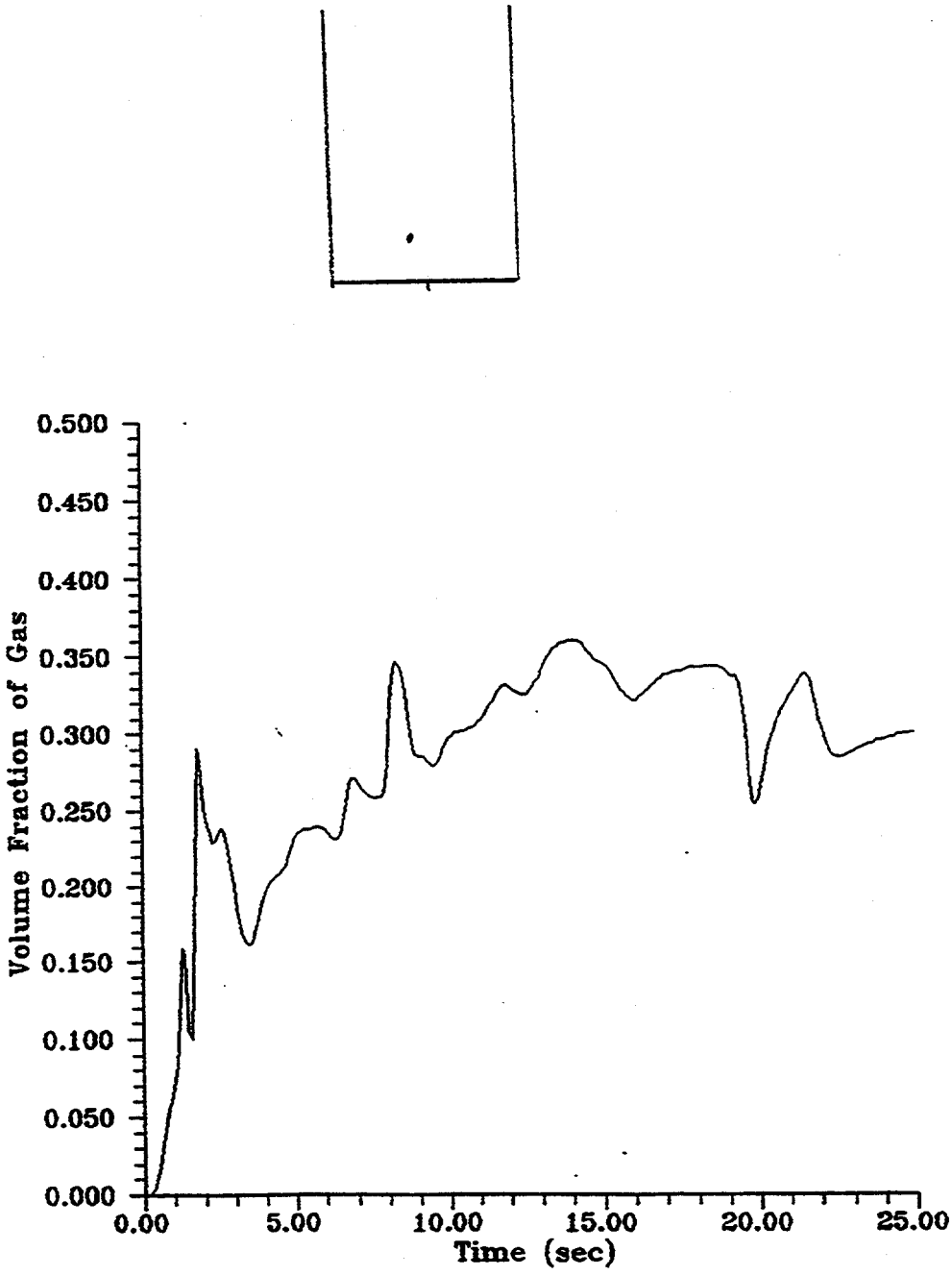

Figure 4.19. Computational data of Fluctuation of Bubble at X=13.20 cm and Y=12 cm for Gas-Liquid-Solid System

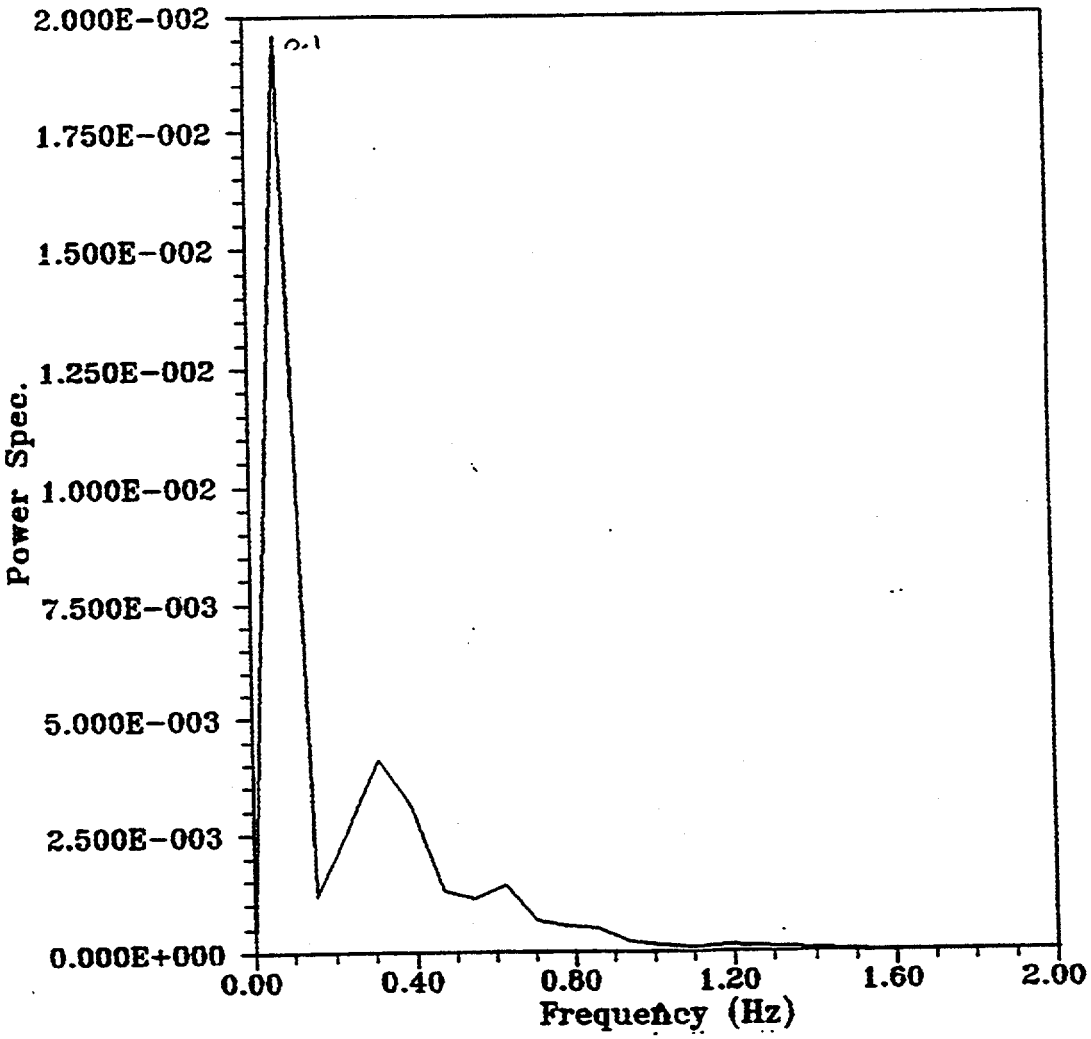

Figure 4.20. Porosity Power Spectrum at X=13.20 cm and Y=12 cm for Gas-Liquid-Solid System